Driven vortices in 3D layered superconductors: Dynamical ordering along the c-axis

Alejandro B. Kolton,[1] Daniel Domínguez,[1] Cynthia J. Olson[2] and Niels Grønbech-Jensen[3,4]
[1] *Centro Atómico Bariloche, 8400 S. C. de Bariloche, Rio Negro, Argentina*
[2] *Department of Physics, University of California, Davis, California 95616*
[3] *Department of Applied Science, University of California, Davis, California 95616*
[4] *NERSC, Lawrence Berkeley National Laboratory, Berkeley, California 94720*

(February 6, 2008)

We study a 3D model of driven vortices in weakly coupled layered superconductors with strong pinning. Above the critical force F_c, we find a plastic flow regime in which pancakes in different layers are uncoupled, corresponding to a *pancake gas*. At a higher F, there is an "smectic flow" regime with short-range interlayer order, corresponding to an entangled *line liquid*. Later, the transverse displacements freeze and vortices become correlated along the c-axis, resulting in a *transverse solid*. Finally, at a force F_s the longitudinal displacements freeze and we find a *coherent solid* of rigid lines.

PACS numbers: 74.60.Ge, 74.40.+k, 05.70.Fh

It is well-known that an external current can induce an ordering of the vortex structure in superconductors with pinning [1]. For a long time, it was believed that the high-current phase would have crystalline order. Recently, it has been found that different kinds of order are possible at high currents, depending on pinning strength and dimensionality [2–7]. This has led to numerous theoretical [2,3], experimental [4] and numerical studies [5–7]. A crystal-like structure, which could be either a perfect crystal [2] or a Bragg glass [3], is only possible in $d = 3$ at large drives. In $d = 2$, or in $d = 3$ for intermediate currents, a transverse glass is expected, with order only in the direction perpendicular to the driving force [3,6,7]. In the equilibrium vortex phase diagram, the behavior of vortex line correlations along the direction of the magnetic field (c-axis) has been intensively discussed both experimentally [8] and theoretically [9]. In the case of driven vortices, little is known on how the c-axis line correlations would behave in the different dynamical regimes. Here we will address this issue starting from the less favorable case: weakly coupled superconducting planes with strong pinning. We will show how the order along the c-axis and the in-plane structural order take place in a sequence of dynamical phases upon increasing current.

We study pancake vortices in a layered superconductor, considering the long-range magnetic interactions between all the pancakes and neglecting Josephson coupling [10]. This model is adequate when the interlayer periodicity d is much smaller than the in-plane penetration length $\lambda_\parallel$ [10]. Previous simulations of driven vortices in 3D superconductors have been performed using Langevin dynamics of short-range interacting particles [11] or the driven isotropic 3D XY model [12].

The equation of motion for a pancake located in position $\mathbf{R}_i = (\mathbf{r}_i, z_i) = (x_i, y_i, n_i d)$, ($\mathbf{z} \equiv \hat{c}$), is:

$$\eta \frac{d\mathbf{r_i}}{dt} = \sum_{j \neq i} \mathbf{F_v}(\rho_{ij}, z_{ij}) + \sum_{p} \mathbf{F_p}(\rho_{ip}) + \mathbf{F} , \qquad (1)$$

where $\rho_{ij} = |\mathbf{r}_i - \mathbf{r}_j|$ and $z_{ij} = |z_i - z_j|$ are the in-plane and inter-plane distance between pancakes i, j, $\rho_{ip} = |\mathbf{r}_i - \mathbf{r}_p|$ is the in-plane distance between the vortex i and a pinning site at $\mathbf{R_p} = (\mathbf{r}_p, z_i)$, η is the Bardeen-Stephen friction, and $\mathbf{F} = \frac{\Phi_0}{c}\mathbf{J} \times \mathbf{z}$ is the driving force due to an in-plane current $\mathbf{J}$. We consider a random uniform distribution of attractive pinning centers in each layer with $\mathbf{F_p} = -2A_p e^{-(\rho/a_p)^2}\mathbf{r}/a_p^2$, where a_p is the pinning range. The magnetic interaction between pancakes $\mathbf{F}_v(\rho, z) = F_\rho(\rho, z)\hat{r}$ is given by [10,13]:

$$F_\rho(\rho, 0) = \frac{A_v}{\rho}\left[1 - \frac{\lambda_\parallel}{\Lambda}\left(1 - e^{-\rho/\lambda_\parallel}\right)\right] \qquad (2)$$

$$F_\rho(\rho, z_n) = -\frac{\lambda_\parallel}{\Lambda}\frac{A_v}{\rho}\left[e^{-|z_n|/\lambda_\parallel} - e^{-R_n/\lambda_\parallel}\right] . \qquad (3)$$

Here, $R = \sqrt{z^2 + \rho^2}$ and $\Lambda = 2\lambda_\parallel^2/d$ is the 2D thin-film screening length. An analogous model to Eqs. (2-3) was used in [14]. We normalize length scales by $\lambda_\parallel$, energy scales by $A_v = \phi_0^2/4\pi^2\Lambda$, and time is normalized by $\tau = \eta\lambda_\parallel^2/A_v$. We consider N_v pancake vortices and N_p pinning centers per layer in N_l rectangular layers of size $L_x \times L_y$, and the normalized vortex density is $n_v = B\,\lambda_\parallel^2/\Phi_0 = (a_0/\lambda_\parallel)^2$. We consider $n_v = 0.29$ with $L_y = 16\lambda_\parallel$ and $L_x = \sqrt{3}/2L_y$, $N_l = 8$ and $N_v = 64$. We take a pinning range of $a_p = 0.2$, a large pinning strengh of $A_p/A_v = 0.2$, with a high density of pinning centers $n_p = 3.125n_v$. The model of Eq.(2-3) is valid in the limit $d \ll \lambda_\parallel \ll \Lambda$. We take $d/\lambda_\parallel = 0.01$, which corresponds to BSCCO compounds [10]. Moving pancake vortices induce a total electric field $\mathbf{E} = \frac{B}{c}\mathbf{v} \times \mathbf{z}$, with $\mathbf{v} = \frac{1}{N_v N_l}\sum_i \mathbf{v}_i$. We study the dynamical regimes in the velocity-force curve at $T = 0$, solving Eq. (1) for increasing values of $\mathbf{F} = F\mathbf{y}$ [13]. We use periodic boundary conditions both in the planes and in the z direction and interactions between all pancakes in all layers are considered [13]. The periodic long-range in-plane and inter-plane interaction is evaluated using Ref. [15]. The equations are integrated with a time step of $\Delta t = 0.01\tau$

and averages are evaluated in 16384 integration steps after 2000 iterations for equilibration. Each simulation is

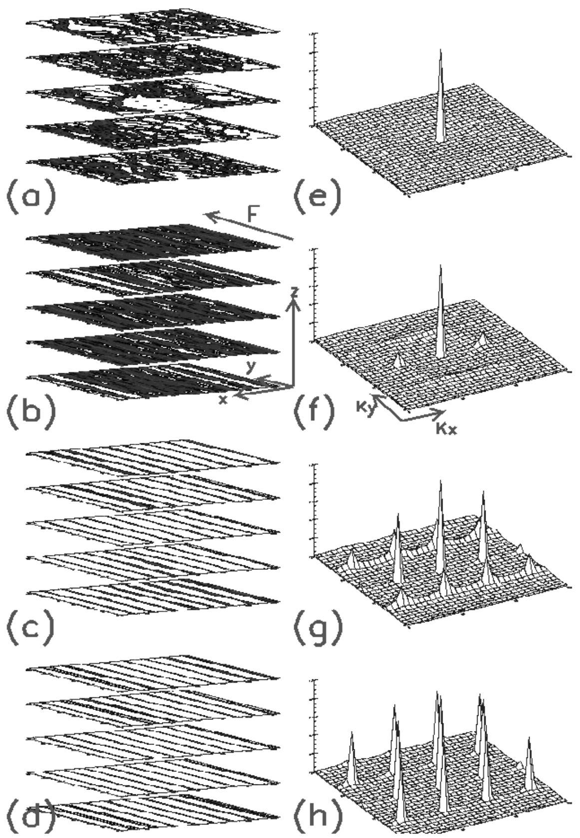

FIG. 1. Vortex trajectories in the first five layers: (a) F=0.6, (b) F=1.1, (c) F=2.0. (d) F=3.9. Surface intensity plot of the averaged in-plane structure factor S($\mathbf{k}$): (e) F=0.6, (f) F=1.1, (g) F=2.0. (h) F=3.9.

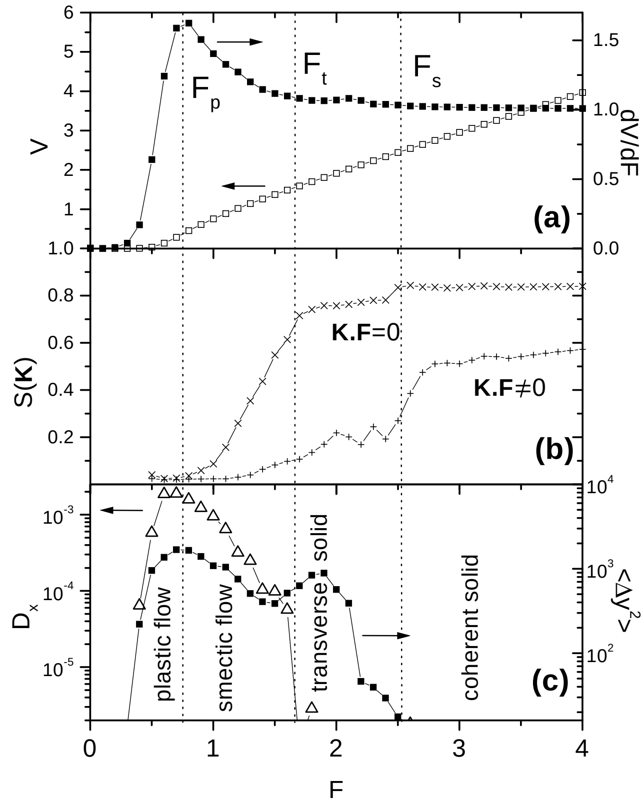

FIG. 2. (a) Velocity-force curve, left scale, black points, dV/dF (differential resistance), right scale, white points. (b) Intensity of the Bragg peaks. For smectic ordering $S(G_1)$, $K_y = 0$, ($\times$) symbols. For longitudinal ordering $S(G_{2,3})$, $K_y \neq 0$, (+) symbols. (c) Diffusion coefficient for transverse motion D_x, ($\triangle$), left scale. Longitudinal displacements $\langle[\Delta y(t)]^2\rangle$ for a given t as a function of F, ($\blacksquare$), right scale.

started at $F = 0$ with a triangular vortex lattice and slowly increasing the force in steps of $\Delta F = 0.1$ up to values as high as $F = 8$.

We start with a qualitative description of the different steady states that arise as a function of increasing force. In Figure 1(a-d) we show the vortex trajectories $\{\mathbf{R}_i(t)\}$ for typical values of F by plotting the positions of the pancakes in five of the layers for all t. In Fig.1(e-h) we show the average in-plane structure factor $S(\mathbf{k}) = \langle \frac{1}{N_l}\sum_n |\frac{1}{N_v}\sum_i \exp[i\mathbf{k}\cdot\mathbf{r}_{ni}(t)]|^2\rangle$, with $\mathbf{k} = (k_x, k_y)$. Above the depinning critical force F_c, we find the following dynamical phases. (i) *Plastic flow* ($F_c < F < F_p$): Pancakes flow in an intrincate network of "plastic" channels similar to the behavior found in 2D [5,7]. The motion in different planes is completely uncorrelated, [Fig.1(a)] and there is no signature of order in the structure factor [Fig.1(e)]. (ii) *Smectic flow* ($F_p < F < F_t$): The motion organizes in "elastic" channels that are almost parallel and separated by a distance $\sim a_0$, see Fig.1(b). Small and broad "smectic" peaks appear in $S(\mathbf{k})$ for $\mathbf{k}\cdot\mathbf{F} = 0$ [Fig.1(f)]. There are "activated" jumps of pancakes between channels. Along the each other between neighboring planes. (iii) *Transverse solid* ($F_t < F < F_s$): There are well defined channels in all the planes and the pancakes do not jump between channels [Fig.1(c)]. The structure factor has sharp smectic peaks and small "longitudinal" peaks ($\mathbf{k}\cdot\mathbf{F} \neq 0$) have appeared [Fig.1(g)]. The location of channels is correlated in the c-axis. (iv) *Coherent solid* ($F > F_s$): The channels become more straigth with small transverse wandering [Fig.1(d)]. The $S(\mathbf{k})$ shows well defined peaks for all $\mathbf{k}$ in the reciprocal lattice [Fig.1(h)]. The dynamical phases (i)-(iii) are similar to the ones found previously in 2D thin films [7].

The characteristic forces F_c, F_p, F_t, F_s separating the different dynamical phases are obtained from the analysis of the in-plane and out of plane structural and dynamical correlations. We show in Fig.2 the in-plane structure factor and temporal fluctuations, obtained in the same way as for 2D [7]. In Fig.2(a) we plot the average velocity $V = \langle V_y(t)\rangle = \langle \frac{1}{N_v N_l}\sum_{n,i}\frac{dy_{ni}}{dt}\rangle$, in the direction of the force as a function of F and its corresponding derivative

dV/dF (differential resistance). The force F_p corresponds to the peak in the differential resistance. We also see a small second maximum in dV/dF for a force between F_t and F_s [16]. In Fig.2(b) we plot the magnitude of the peaks in the in-plane structure factor. We show the peak height at $G_1 = 2\pi/a_0\hat{x}$, corresponding to smectic ordering, and the average of the peaks corresponding to longitudinal ordering at $\mathbf{G}_2 = \pm 2\pi/a_0(1/2, \sqrt{3}/2)$ and $\mathbf{G}_3 = \pm 2\pi/a_0(-1/2, \sqrt{3}/2)$. We see that at F_p the smectic peak rises up from zero, then at F_t it reaches an almost constant value and later at F_s it has a small jump. The longitudinal peak has a small finite value for forces above F_p, and only at F_s shows a significant increment towards a large value. Comparing with the previous 2D results [7], we can make the reasonable assumption that for $F_p < F < F_t$ there is only short-range smectic order (since there is activated transverse diffusion beteween elastic channels, see below), for $F_t < F < F_s$ there is probably quasi-long range smectic order but short range longitudinal order, and above F_s there is both transversal and longitudinal order (quasilong-range or long-range). What is new, compared with the 2D thin film case [7], is that above a force F_s there is a significant amount of longitudinal order. This may correspond either to a moving crystalline phase (if there is long-range order) or to a moving Bragg glass (if there is quasilong-range order) [3]. We have verified that, for a given $F > F_s$, there is both longitudinal and transversal order for system sizes of $N_l \times N_v = 5 \times 36, 5 \times 64, 8 \times 64, 8 \times 100, 10 \times 100$. However, a detailed finite size analysis is not possible with these few small samples. We complement our discussion of the in-plane physics with the study of the temporal fluctuations, which are shown in Fig.2(c). We calculate the transverse diffusion coefficient D_x from the average quadratic transverse displacements of vortices from their center of mass position $(\bar{X}_n, \bar{Y}_n)$, $\frac{1}{N_v N_l}\sum_i [x_i(t) - \bar{X}_{n_i}(t) - x_i(0) + \bar{X}_{n_i}(0)]^2 \approx D_x t$. We find that D_x is maximum at F_p in coincidence with the peak in dV/dF. Below F_p diffusion is through the intricate network of plastic channels, above F_p diffusion is through activated jumps between elastic channels. D_x sharply drops to zero at F_t, indicating that transverse displacements are localized in the *transverse solid* phase [7]. The drift from the center of mass of longitudinal displacements $\langle[\Delta y(t)]^2\rangle = \langle[y_i(t) - \bar{Y}_{n_i}(t) - y_i(0) + \bar{Y}_{n_i}(0)]^2\rangle$ is superdiffusive for $F < F_s$, similar to the results observed in 2D films [7]. For $F > F_s$ the longitudinal displacements become frozen in a constant value $\langle[\Delta y(t)]^2\rangle < a_0/N_l$, as it is shown in Fig.2(c). Since in-plane displacements are localized and there are large transversal and longitudinal Bragg peaks, we call this phase a *coherent solid*.

Let us now discuss how the ordering along the c-axis takes place. We analyze the pair distribution function: $g(\rho, n) = \frac{L_x L_y}{N_v}\langle\sum_{i \neq j}\delta(\rho - \rho_{ij})\delta_{n,n_{ij}}\rangle$. From $g(\rho, n)$ we define a correlation function along c-axis $C_z(n) =$

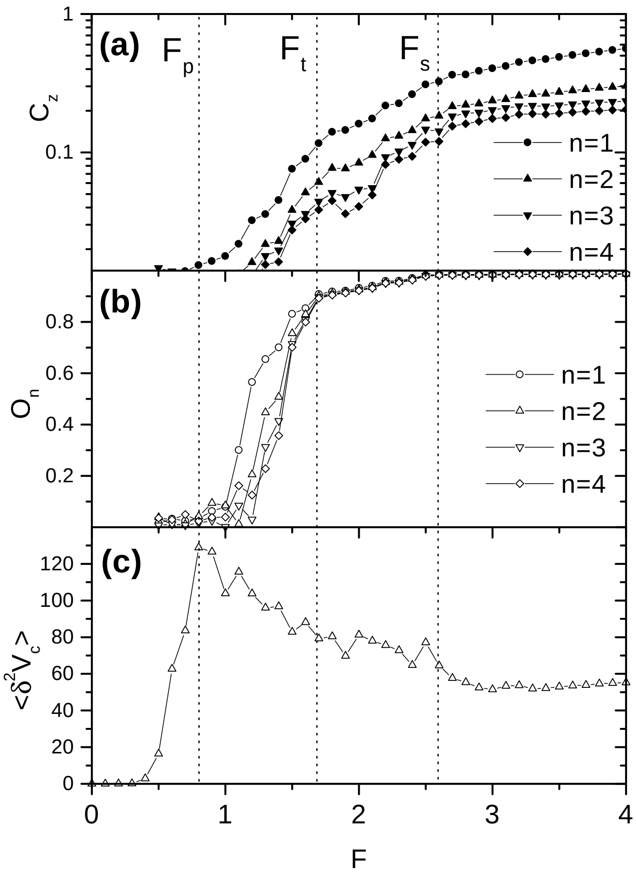

FIG. 3. (a) Correlation parameter in c-direction of instantaneous configurations $C_z(n)$ vs F for $n = 1, 2, 3, 4$ interplane distance. (b) Trajectories overlap correlation parameter in c-direction O_n vs F for $n = 1, 2, 3, 4$ interplane distance. (c) Voltage fluctuations in c-direction $\langle\delta^2 V_c\rangle$ vs F.

finite $C_z(n = 1)$, meaning that pancakes in neighboring planes are coupled and a "vortex line" can therefore be defined. In principle, an exponential decay $C_z(n) \sim \exp(-n/\xi_z)$ would define a correlation length for the vortex line [9]. On the other hand, long-range ordering will be given by $C_z(n \to \infty) \to C_z^\infty > 0$. In Fig.3(a) we show $C_z(n)$ as a function of F for $n = 1, 2, 3, 4$. We see that at F_p there is an onset of short-range order along the c-axis with a finite $C_z(n = 1)$. At higher forces between F_p and F_t the other $C_z(n > 1)$ start to rise. The absence of correlations for $F < F_p$ means that pancake motion is completely random and uncorrelated between different planes. Therefore, we propose that the plastic flow regime corresponds to a *pancake gas*. Above F_p, in the smectic flow regime, it is possible to define a vortex line with short range correlations along the c-axis. Since there are in-plane jumps between elastic channels (i.e., cutting and reconnection of flux lines) we may consider this phase as an entangled *line liquid*. Above F_t, $C_z(n)$ is finite for all n considered and tends to saturate upon

increasing n. This indicates that vortex lines become more stiff above F_t. We also analyzed the c-axis correlation between averaged vortex densities. We first define $\rho_v(\mathbf{r},n,t) = \frac{1}{N_v}\sum_i \delta(\mathbf{r}-\mathbf{r}_{ni}(t))$ taking a coarse-graining scale $\Delta r = a_0/2$ (results do not vary much for $\Delta r = a_0/4$). The regions where the average density $\langle \rho_v(\mathbf{r},n)\rangle$ is large define the paths of steady state vortex motion. We can thereby calculate the overlap function of vortex trajectories between different planes as $O_n = C_\rho(n)/C_\rho(0)$, with $C_\rho(n) = \frac{L_x L_y}{N_l}[\sum_m \int d\mathbf{r}\langle\rho_v(\mathbf{r},m)\rangle\langle\rho_v(\mathbf{r},m+n)\rangle]-1$. This is shown in Fig.3(b). We see that O_n also has an onset at F_p. For $F_p < F < F_t$, we have some overlap of the elastic channels that decreases with increasing n, consistent with the entangled line-liquid picture. More interestingly, at F_t the overlap function O_n becomes independent of n. This means that there is long-range c-axis coupling of the path of the elastic channels. When transverse displacements become localized in the x-direction, they also become locked in the c-direction. Thus, the freezing of in-plane transverse displacements occurs simultaneously with a transverse disentanglement of flux lines at F_t. A striking result is that we find $O_n \approx 1$ above F_s, i.e., a perfect c-axis coupling of elastic channels (within the scale $\sim a_0/4$). Another interesting point to consider is the correlation of vortex velocities. If vortices in different planes move at different velocities, they will induce a Josephson voltage difference along the c-axis given by $V_{n,n+1}(\mathbf{r},t) = \frac{\Phi_0}{2\pi c}\frac{d}{dt}\phi_{n,n+1}(\mathbf{r},t)$, with $\phi_{n,n+1}$ the superconducting phase difference between planes n and $n+1$. A good approximation for pancakes at $\mathbf{r}_{n,i}$ is to write $\phi_{n,n+1}(\mathbf{r},t) = \sum_i[f(\mathbf{r}-\mathbf{r}_{n,i}) - f(\mathbf{r}-\mathbf{r}_{n+1,i})]$ with $f(\mathbf{r}) \approx \arctan(x/y)$. We can therefore estimate the c-axis voltage fluctuations as $\langle\delta^2 V_c\rangle = \sum_n \int[\langle V^2_{n,n+1}(\mathbf{r},t)\rangle - \langle V_{n,n+1}(\mathbf{r},t)\rangle^2]d\mathbf{r} \approx A\sum_n[\langle\mathbf{V}_n^2\rangle - \langle\mathbf{V}_n\rangle^2] - [\langle\mathbf{V}_n\cdot\mathbf{V}_{n+1}\rangle - \langle\mathbf{V}_n\rangle\cdot\langle\mathbf{V}_{n+1}\rangle]$; with $\mathbf{V}_n(t) = \frac{1}{N_v}\sum_i \mathbf{v}_{n,i}(t)$, and the constant $A \sim \log\Lambda$ if $L > \Lambda$ or $A \sim \log(L)$ otherwise. It is clear that $\langle\delta^2 V_c\rangle = 0$ for pancakes moving with the same velocity in all planes. We see in Fig.3(c) that the voltage fluctuations have a maximum at F_p. For $F > F_p$, $\langle\delta^2 V_c\rangle$ decreases, and above F_s it reaches an almost F-independent value. The fact that $\langle\delta^2 V_c\rangle$ does not vanish above F_s is consistent with the result that $C_z(n) < 1$ for all values of F in Fig.3(a). In other words, while transverse displacements are strongly correlated along the c direction for large forces [Fig.3(b)], the longitudinal displacements in different planes are weakly correlated .

In conclusion, we have clearly distinguished different dynamical phases in 3D layered superconductors considering both in-plane and c-axis ordering [16]. The onset of short-range c-axis correlations could be studied experimentally with plasma resonance measurements [17]. The long-range ordering along the c-axis could be studied through simultaneous measurements of ρ_c resistivity and in-plane current-voltage response [18].

We acknowledge discussions with L.N. Bulaevskii, P.S. Cornaglia, F. de la Cruz, Y. Fasano, M. Menghini. This work has been supported by ANPCYT (Proy. 03-00000-01034), by Fundación Antorchas (Proy. A-13532/1-96), Conicet, CNEA and FOMEC (Argentina); by CLC and CULAR (Los Alamos), and by the Director, Office of Adv. Sci. Comp. Res., Division of Mathematical, Information, and Computational Sciences of the U.S.D.O.E. (contract number DE-AC03-76SF00098).

---

[1] R. Thorel *et al.*, J. Phys. (Paris) **34**, 447 (1973)

[2] A. E. Koshelev and V. M. Vinokur, Phys. Rev. Lett. **73**, 3580 (1994).

[3] T. Giamarchi and P. Le Doussal, Phys. Rev. Lett. **76**, 3408 (1996); P. Le Doussal and T. Giamarchi, Phys. Rev. B **57**, 11356 (1998); L. Balents, M. C. Marchetti and L. Radzihovsky, *ibid.* **57**, 7705 (1998); S. Scheidl and V. M. Vinokur, *ibid.* **57**, 13800 (1998).

[4] S. Bhattacharya and M. J. Higgins, Phys. Rev. Lett. **70**, 2617 (1993); M. C. Hellerqvist *et al.*, *ibid.* **76**, 4022 (1996); U. Yaron *et al.*, Nature (London) **376**, 743 (1995); F. Pardo *et al*, *ibid.* **396**, 348 (1998).

[5] H. J. Jensen *et al.*, Phys. Rev. Lett. **60**, 1676 (1988); A.-C. Shi and A. J. Berlinsky, *ibid.* **67**, 1926 (1991). N. Grønbech-Jensen, A. R. Bishop and D. Domínguez, *ibid.* **76**, 2985 (1996); C. J. Olson, C. Reichhardt and F. Nori, *ibid.* **80**, 2197 (1998).

[6] K. Moon, R. T. Scalettar and G. Zimányi, Phys. Rev. Lett. **77**, 2778 (1996); S. Ryu *et al.*, *ibid.* **77**, 5114 (1996). S. Spencer and H. J. Jensen, Phys. Rev. B **55**, 8473 (1997); C. J. Olson, C. Reichhardt and F. Nori, Phys. Rev. Lett. **81**, 3757 (1998); D. Domínguez, *ibid.* **82**, 181 (1999).

[7] A. B. Kolton, D. Domínguez, N. Grønbech-Jensen, Phys. Rev. Lett. **83**, 3061 (1999).

[8] D. López *et al.*, Phys. Rev. Lett. **76**, 4034 (1996).

[9] See for example P. Olsson and S. Teitel, Phys. Rev. Lett. **82**, 2183 (1999) and references therein.

[10] J. R. Clem, Phys. Rev. B. **43**, 7837 (1991).

[11] S. Ryu, D. Stroud, Phys. Rev. B, **54**, 1320 (1996); N. K. Wilkin, H. J. Jensen, Phys. Rev. Lett. **21**, 4254 (1997); A. van Otterlo, R. T. Scalettar, G. T. Zimámyi, *ibid.* **81**, 1497 (1998); C. J. Olson, R. T. Scalettar, G. T. Zimányi, cond-mat/9909454.

[12] D. Domínguez, N. Grønbech-Jensen and A.R. Bishop, Phys. Rev. Lett. **78**, 2644 (1997).

[13] A. B. Kolton, D. Domínguez and N. Grønbech-Jensen, Physica C, to be published; C. J. Olson and N. Grønbech-Jensen, Physica C, to be published.

[14] D. Reefman, H. B. Brom, Physica C **213**, 229 (1993).

[15] N. Grønbech-Jensen, Int. J. Mod. Phys. C **7**, 873 (1996); Comp. Phys. Comm. **119**, 115 (1999).

[16] For weak pinning, the ordering transition in the c-axis may occur in a single step and also a pronounced second peak in dV/dF is observed, see C. J. Olson, N. Grønbech-Jensen, A. B. Kolton and G. T. Zimányi, preprint.

[17] O. Tsui *et al.*, Phys. Rev. Lett. **73**, 724 (1994); L. Bulaevskii, M. Maley and M. Tachiki, *ibid.* **74**, 801 (1994).
[18] M. Menghini *et al.*, unpublished.